



Article

Genome-Wide Identification and Expression Analysis of the Stearoyl-Acyl Carrier Protein $\Delta 9$ Desaturase Gene Family under Abiotic Stress in Barley

Mingyu Ding¹, Danni Zhou¹, Yichen Ye¹, Shuting Wen¹, Xian Zhang^{1,2}, Quanxiang Tian^{1,2}, Xiaoqin Zhang^{1,2}, Wangshu Mou^{1,2}, Cong Dang^{1,2}, Yunxia Fang^{1,2} and Dawei Xue^{1,2,*} 

¹ College of Life and Environmental Sciences, Hangzhou Normal University, Hangzhou 311121, China; ding514019@163.com (M.D.); zzz20211218@163.com (D.Z.); yeyichende@outlook.com (Y.Y.); stwen2468@163.com (S.W.); zhangxian@hznu.edu.cn (X.Z.); quanxiang@hznu.edu.cn (Q.T.); zxq@hznu.edu.cn (X.Z.); mwsdiana@163.com (W.M.); dangcong@hznu.edu.cn (C.D.); yxfang12@163.com (Y.F.)

² Zhejiang Provincial Key Laboratory for Genetic Improvement and Quality Control of Medicinal Plants, Hangzhou Normal University, Hangzhou 311121, China

* Correspondence: dwxue@hznu.edu.cn

Abstract: Stearoyl-acyl carrier protein (ACP) $\Delta 9$ desaturase (SAD) is a critical fatty acid dehydrogenase in plants, playing a prominent role in regulating the synthesis of unsaturated fatty acids (UFAs) and having a significant impact on plant growth and development. In this study, we conducted a comprehensive genomic analysis of the SAD family in barley (*Hordeum vulgare* L.), identifying 14 HvSADs with the FA_desaturase_2 domain, which were divided into four subgroups based on sequence composition and phylogenetic analysis, with members of the same subgroup possessing similar genes and motif structures. Gene replication analysis suggested that tandem and segmental duplication may be the major reasons for the expansion of the SAD family in barley. The promoters of HvSADs contained various *cis*-regulatory elements (CREs) related to light, abscisic acid (ABA), and methyl jasmonate (MeJA). In addition, expression analysis indicated that HvSADs exhibit multiple tissue expression patterns in barley as well as different response characteristics under three abiotic stresses: salt, drought, and cold. Briefly, this evolutionary and expression analysis of HvSADs provides insight into the biological functions of barley, supporting a comprehensive analysis of the regulatory mechanisms of oil biosynthesis and metabolism in plants under abiotic stress.

Keywords: barley; SAD; evolution; unsaturated fatty acids (UFAs); abiotic stress



Citation: Ding, M.; Zhou, D.; Ye, Y.; Wen, S.; Zhang, X.; Tian, Q.; Zhang, X.; Mou, W.; Dang, C.; Fang, Y.; et al. Genome-Wide Identification and Expression Analysis of the Stearoyl-Acyl Carrier Protein $\Delta 9$ Desaturase Gene Family under Abiotic Stress in Barley. *Int. J. Mol. Sci.* **2024**, *25*, 113. <https://doi.org/10.3390/ijms25010113>

Academic Editor: Gábor Kocsy

Received: 24 October 2023

Revised: 11 December 2023

Accepted: 18 December 2023

Published: 21 December 2023



Copyright: © 2023 by the authors. Licensee MDPI, Basel, Switzerland. This article is an open access article distributed under the terms and conditions of the Creative Commons Attribution (CC BY) license (<https://creativecommons.org/licenses/by/4.0/>).

1. Introduction

The unsaturated fatty acids (UFAs) are produced through a series of desaturation and elongation processes of saturated fatty acids, which are a highly sophisticated mechanism in plants. Stearoyl-acyl carrier protein (ACP) $\Delta 9$ desaturase (SAD) is a decisive enzyme located in the plastid, catalyzing the dehydrogenation of stearic acid (C18:0) at a specific position in the fatty acid chain to form a double bond for the first step of desaturation, resulting in the formation of monounsaturated fatty acid (C18:1) [1,2]. Hence, SAD directly determines the ratio of saturated fatty acids to UFAs in plant oils [3]. Oleic acid, as the main form of monosaturated fatty acid exported by plastids, can be further desaturated into polyunsaturated fatty acid derivatives and used as a main component of the cell membrane system in the form of phospholipids [4].

Fatty acids and their derivatives are important energy-storage substances and are the main components of cell membrane lipids in plants. They are particularly actively synthesized during seed development and have been validated in most species. *GmSAD5* is highly expressed in soybeans during the middle and late stages of seed development,

consistent with the oil enrichment period. It was found to have strong selectivity for stearic acid substrates and could efficiently catalyze the biosynthesis of monounsaturated oleic acid [5]. Expression analysis showed that *GhA-SAD6* and *GhD-SAD8* in cotton are preferentially generated during endosperm development and are responsible for producing palmitoleic acid in cotton seed oil [6]. Four *SAD*-encoding genes (*FAB2*, *AAD5*, *AAD1*, and *AAD6*) in *Arabidopsis* are also transcriptionally induced in seeds, where *FAB2*, *AAD5*, and *AAD1* are involved in the formation of the embryonic corneum [7]. Interestingly, *TcSAD1* in cacao is universally expressed in all the tissues and is highly correlated with dramatic changes in fatty acid composition during seed maturation [8]. Overall, these results support that various *SADs* in these plants are intimately linked to the lipid synthesis pathway and seed development.

Fatty acids and their derivatives are extensively involved in regulating various defense pathways such as basal immunity, effector-induced resistance, and systemic resistance. Research has found that endoplasmic reticulum membranes of oilseed rape grown at low temperatures (4 °C) are rich in polyunsaturated fatty acids and have a significantly altered lipid composition. Additionally, an allele of *SAD*, homologous to *AtSAD6* (*At1g43800*), was also found to be responsive to, and up-regulated by, low temperatures in oilseed rape [9]. The overexpression of the *ScoSAD* prominently improved the freezing resistance of transgenic potato plants [10]. The transcription levels of soybean *SAD* and *FAD2-1* were markedly increased under low-temperature treatment. Additionally, the transcription level of *FAD2-1B* was also higher than that of *FAD2-1A* after 35 days of flowering [11]. Treating peanut seedlings with 250 mM of NaCl weakened the activity of ω -3 fatty acid desaturase, leading to decreased contents of UFAs, which affected the stability and fluidity of the membrane and even caused irreversible damage to the plant. On the contrary, increasing the content of UFAs contributed to the improvement of salt tolerance in *Suaeda salsa* [12–14]. Apart from responding positively to temperature, drought, and salt stresses, FAs also serve defense purposes by affecting hormone levels. Low oleic acid induced the accumulation of salicylic acid (SA) and activated defense responses in *GhSSI2s*-silenced cotton to resist disease, whereas the disruption of *GhSSI2s* directly activated resistance gene-dependent defenses [15]. In addition, UFAs reacted immediately with reactive oxygen species (ROS) to maintain the stability of the cytomembrane and organelle membranes by regulating ROS levels [16–18]. Given the important role of FAs in regulating metabolic homeostasis and ensuring normal plant growth, this study explores the bioinformatics aspects of *SAD*.

Barley is the fourth largest cereal crop in the world after wheat, rice, and maize [19]. The analysis and publication of the barley genome have facilitated high-resolution, precision genomics research, and studying specific gene families in barley can help elucidate the molecular genetic mechanisms of wheat crops. A significant number of gene families have been identified in barley [20–26], but systematic research on the *SADs* encoding FA dehydrogenase in barley has not yet been reported. This study screened the barley *SAD* family based on database data to confirm 14 members distributed on four chromosomes, with relatively conservative protein motifs. This study focuses on 14 *HvSADs* and investigates their expression under abiotic stress using bioinformatics analysis, with a view of exploring the excellent resistance function of *SADs* and providing a theoretical basis for genetic improvement and molecular breeding in barley.

2. Results

2.1. Identification and Characterization of *SAD* Proteins in Barley

Through homologous comparison and domain validation, 14 *SADs* were identified in the whole barley genome and designated as *HvSAD1* to *HvSAD14*. The physicochemical properties of the *SADs*, such as the molecular weight (MW), number of amino acids (aa), theoretical isoelectric point (pI), aliphatic index, and other information, are summarized in Table 1. The average protein length of the *HvSADs* was 396 aa, ranging from 339 (*HvSAD12*) to 428 (*HvSAD6*) aa, while the corresponding MWs were 38–47 kDa, with an average of approximately 44 kDa. The average theoretical pI was 7.23, distributed between 5.97

(HvSAD12) and 9.03 (HvSAD7). Half of the HvSADs were acidic, and the rest were alkaline. The aliphatic index of the HvSADs ranged from 72.91 to 87.33, with an average of 79.71. Moreover, all of the HvSADs possessed negative GRAVY values (ranging from -0.177 to -0.490), indicating the hydrophilic character of the HvSADs. The subcellular localization of the proteins showed that most HvSADs were located in chloroplasts, with a few located in the cytoplasm and mitochondria, which is speculated to affect photosynthesis. The variability in the physicochemical properties of the HvSADs may reflect a diverse protein structure and function. All characteristics of the HvSADs are shown in Table 1.

2.2. Sequence Alignment and Phylogenetic Analysis

The sequence alignment results of the HvSADs showed that the overall amino acid similarity among proteins was 57.62%. Different colors were used to visually represent the proportion of homology, with yellow representing 100%, blue representing ≥ 75%, and purple representing ≥ 50%. From Figure 1, it can be observed that the homologous proportion of HvSADs ranging from 50% to 100% accounted for a higher proportion of the total sequence. The black line represents the region of the FA_desaturase_2 domain. The conserved motifs of Motif1, Motif2, Motif3, Motif5, and Motif6 are common components of the domain and may be an important criterion for determining whether the candidate's SADs possess this domain (Figure 1). HvSAD12 was found to have significantly different homologous sequences compared with other members, thereby increasing the difference in the comparison results.

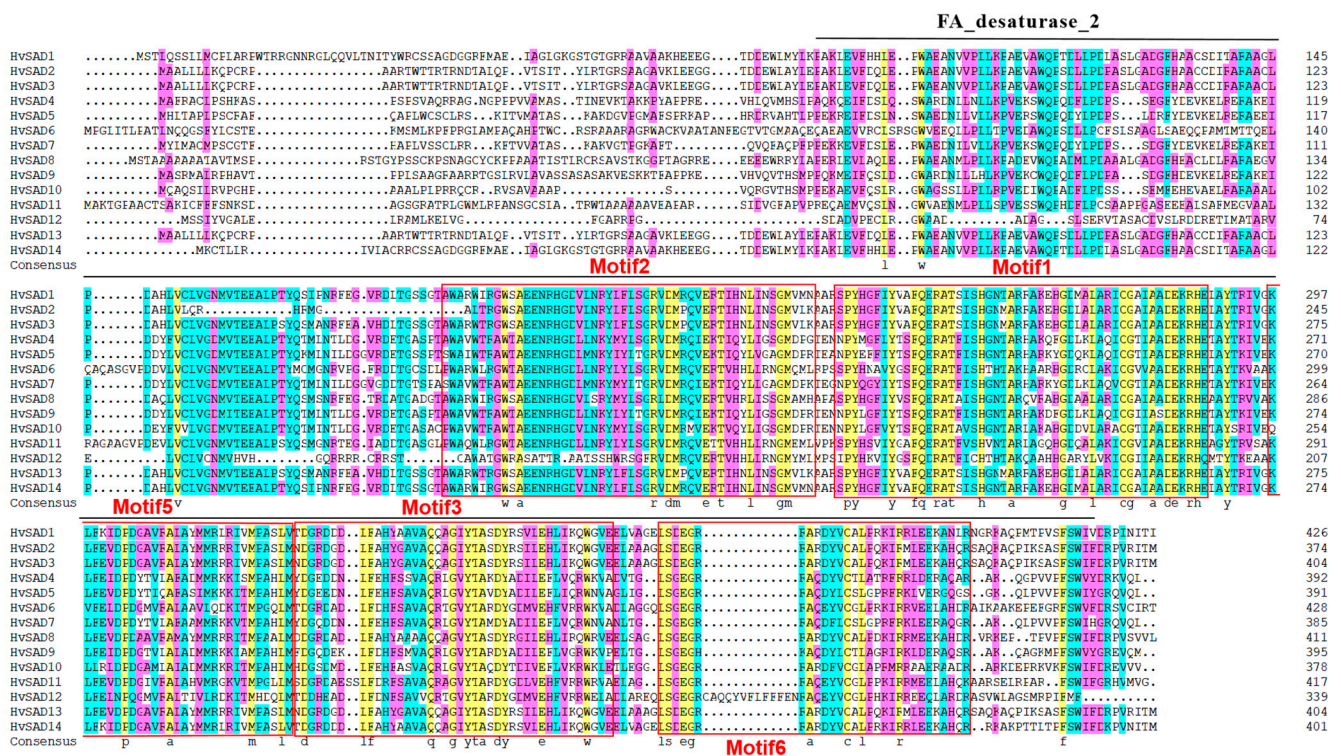


Figure 1. Multiple sequence alignment of HvSADs. Different colors represent different proportions of homology. Yellow represents = 100%, blue represents ≥ 75%, and purple represents ≥ 50%; the black solid line represents the FA_desaturase_2 domain. The range shown in the red box is the common motifs by HvSADs.

Table 1. Detailed information of the identified barley SADs.

Gene Name	Gene ID	Protein				Subcellular Localization	Domain	Chromosome	Genomic Location	
		Size (aa)	MW (Da)	pI	Aliphatic Index					GRAVY
<i>HvSAD1</i>	HORVU.MOREX.r3.2HG0106740	427	47,347	8.47	85.55	−0.267	Chloroplast	FA_desaturase_2	Chr2	23,954,883–23,956,257
<i>HvSAD2</i>	HORVU.MOREX.r3.2HG0101470	375	41,677.74	8.68	87.33	−0.257	Mitochondrial	FA_desaturase_2	Chr2	13,191,866–13,193,197
<i>HvSAD3</i>	HORVU.MOREX.r3.2HG0101440	405	44,883.21	7.19	84.96	−0.241	Mitochondrial	FA_desaturase_2	Chr2	13,111,139–13,112,470
<i>HvSAD4</i>	HORVU.MOREX.r3.2HG0161410	392	44,559.57	6.04	73.44	−0.490	Chloroplast	FA_desaturase_2	Chr2	425,614,894–425,618,180
<i>HvSAD5</i>	HORVU.MOREX.r3.5HG0535350	391	44,667.93	6.05	80.36	−0.405	Chloroplast	FA_desaturase_2	Chr5	581,725,723–581,727,357
<i>HvSAD6</i>	HORVU.MOREX.r3.5HG0486420	428	47,617.36	7.59	73.93	−0.306	Chloroplast	FA_desaturase_2	Chr5	459,736,400–459,738,111
<i>HvSAD7</i>	HORVU.MOREX.r3.5HG0457600	385	43,660.82	5.97	74.75	−0.381	Chloroplast	FA_desaturase_2	Chr5	262,136,160–262,138,788
<i>HvSAD8</i>	HORVU.MOREX.r3.7HG0668240	412	45,390.46	6.87	72.91	−0.344	Chloroplast	FA_desaturase_2	Chr7	103,262,598–103,263,947
<i>HvSAD9</i>	HORVU.MOREX.r3.3HG0310210	395	44,530.92	6.65	78.61	−0.409	Chloroplast	FA_desaturase_2	Chr3	573,217,384–573,221,932
<i>HvSAD10</i>	HORVU.MOREX.r3.3HG0307490	378	42,389.33	6.24	79.29	−0.324	Chloroplast	FA_desaturase_2	Chr3	564,864,759–564,866,328
<i>HvSAD11</i>	HORVU.MOREX.r3.3HG0309010	417	45,352.59	6.87	78.01	−0.177	Chloroplast	FA_desaturase_2	Chr3	569,309,951–569,311,619
<i>HvSAD12</i>	HORVU.MOREX.r3.3HG0288610	339	38,752.42	9.03	76.31	−0.297	Cytoplasmic	FA_desaturase_2	Chr3	484,477,447–484,478,466
<i>HvSAD13</i>	HORVU.MOREX.r3.2HG0101500	405	44,883.21	7.19	84.96	−0.241	Mitochondrial	FA_desaturase_2	Chr2	13,265,580–13,266,911
<i>HvSAD14</i>	HORVU.MOREX.r3.2HG0106840	402	44,563	8.4	85.55	−0.236	Chloroplast	FA_desaturase_2	Chr2	24,197,160–24,198,368

2.3. Phylogenetic Analysis of SAD Proteins

Elucidating phylogenetic relationships is essential for understanding the structure and evolution of gene families. By comparing the SADs of barley, rice, wheat, maize, *A. thaliana*, *G. hirsutum*, *S. lycopersicum*, and *G. max*, we classified HvSADs and their homologs into four groups, namely Class I–Class IV, based on the distance of the genetic relationships (Figure 2). No HvSAD member was distributed in Class I, and most of them were distributed in Class II and Class IV rather than in Class III. HvSAD1 and HvSAD14 are more closely related, and HvSAD2, HvSAD3, and HvSAD13 also belong to the same branch. As a whole, HvSADs are closely associated with homologs in wheat, rice, and maize, and most are not on the same terminal branch as cotton, tomato, and *Arabidopsis*, suggesting higher evolutionary homology with monocotyledonous plants than dicotyledonous plants. Notably, most HvSADs are closely related to AtSAD6 (At1g43800) and do not belong to the same branch as other members of *Arabidopsis*, indicating the possibility that AtSAD6 plays an important role in the evolution of SADs in connecting monocots and dicots.

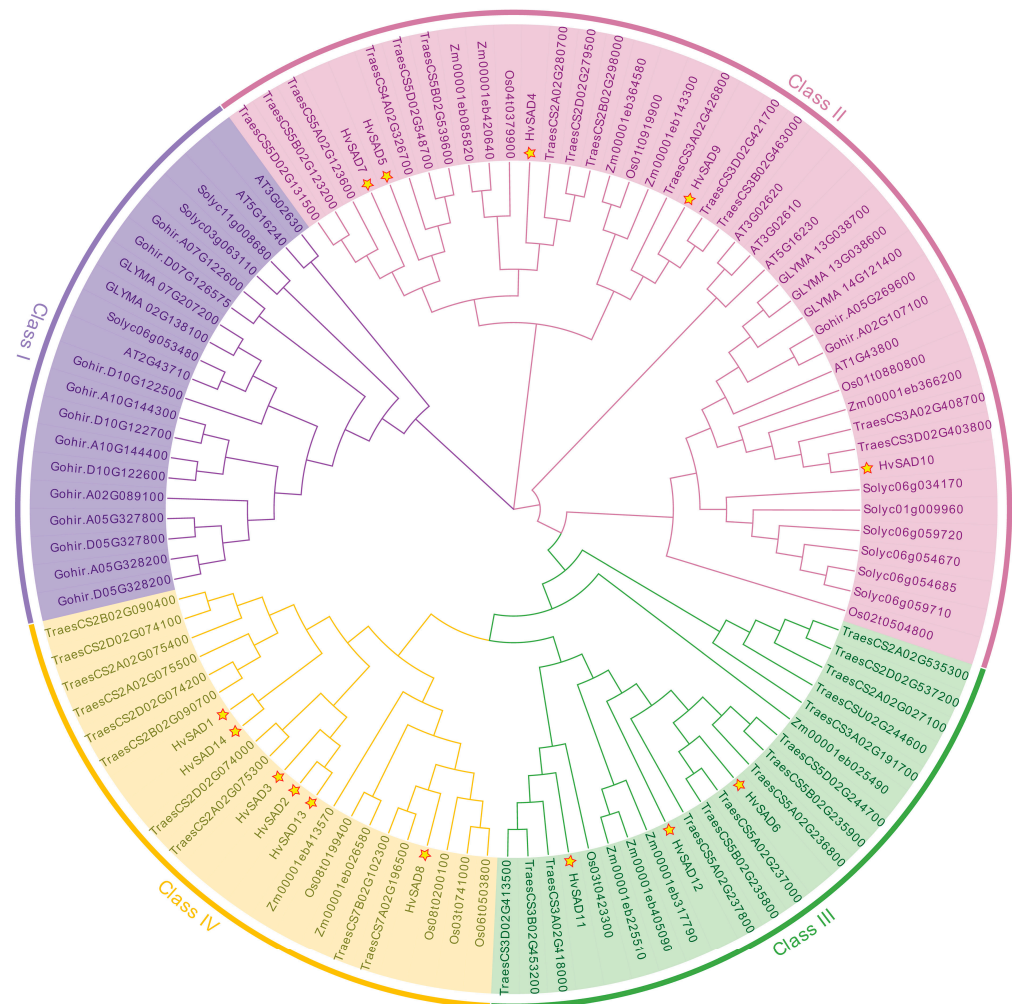


Figure 2. Phylogenetic analysis of HvSADs and their homologs from various organisms. AT represents *A. thaliana*, Zm represents *Z. mays*, Os represents *O. sativa* L, Traes represents *T. aestivum*, GLYMA represents *G. max*, Gohir represents *G. hirsutum*, Soly represents *S. lycopersicum*, and Hv represents *H. vulgare*. The phylogenetic tree was generated using the NJ method by MEGA7; bootstrap values = 1000. SADs are classified into four groups (Class I–IV) and are distinguished by different colors. HvSADs are marked with stars.

2.4. Gene Structure and Protein Motif Analysis of the *HvSADs* Family

To further explore the evolutionary, functional diversity, and domain characteristics of the *HvSADs*, the structural distribution of exons, introns, non-coding regions, and conserved motifs was investigated (Figure 3a, Supplementary Table S2). Ten motifs were identified in *HvSADs*, and the results showed that the rest of the motifs, except for Motif8 and Motif9, were associated with the FA_desaturase_2 domain. *HvSADs* have five common motifs in this domain, whereas the distribution of other motifs is not significantly different, such as Motif7, Motif4, Motif10, and Motif8. It is noteworthy that except for *HvSAD12*, the other members also possess Motif4, Motif7, and Motif10 related to the domain (Figures 1 and 3). In Class IV, except for a lack of Motif4 for *HvSAD2*, all other members have 10 predicted motifs and a concentration of exon regions (Figure 3b).

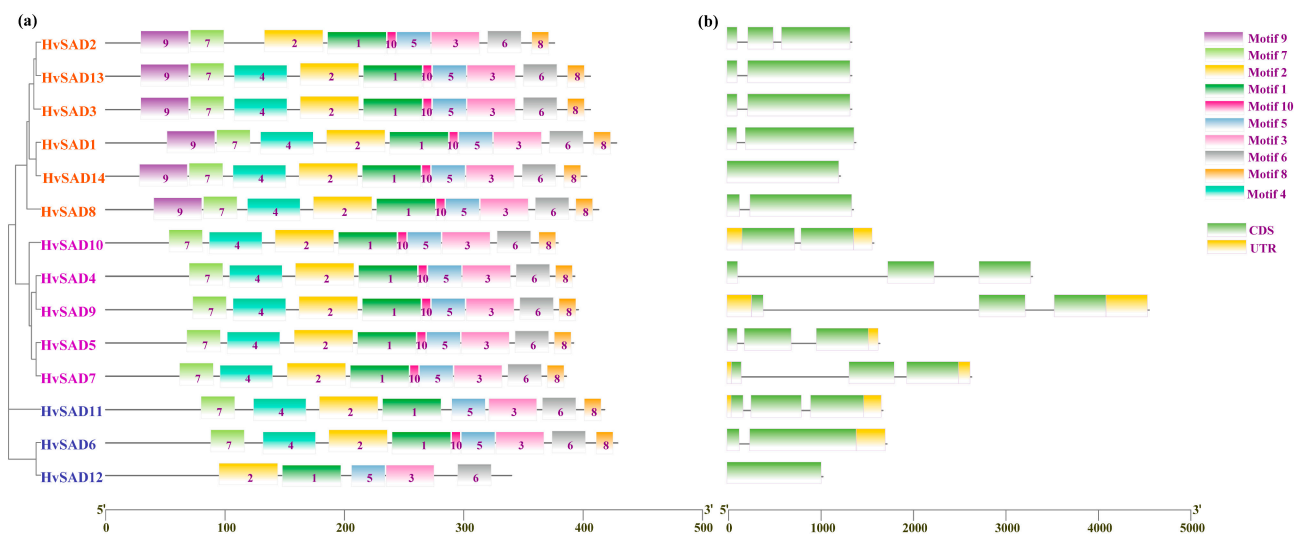


Figure 3. Conserved motifs and gene structures. (a) Motif patterns of *HvSADs*. Boxes with different colors represent various conserved motifs. (b) Exon–intron architectures of *HvSADs*. The introns, exons, and untranslated regions are represented by black lines, green boxes, and yellow boxes, respectively.

The genetic structure composition indicated that *HvSADs* have fewer introns, but the intron composition of *HvSAD4*, *HvSAD7*, and *HvSAD9* is higher compared to other members. In addition, the phylogenetic tree shows a high similarity of gene structures at the end of the same branch and a low similarity of gene structures between branches of different divisions, which may have been in adaptation to the external environment, leading to the diversity of gene families.

2.5. Cis-Regulatory Elements Analysis in the Promoters of *HvSADs*

Plants need to rapidly adapt to the constantly changing environment and ensure timely defense to support their normal growth and development. Understanding the CRE composition of the *HvSAD* promoters can help elucidate the potential factors affecting *HvSAD* expression and the regulatory pathways for participation. The results showed that common CREs (such as TATA-box and CAAT-box) are present in the promoter regions of *HvSADs*. Furthermore, there are many other functional elements (Figure 4), which can be categorized into four groups: (1) growth and development regulation elements, such as zein metabolism regulation-related element (O2-Site) and meristem expression-related element (CAT-box); (2) stress-responsive elements, such as drought-responsive element (MBS), low temperature-responsive element (LTR), and anaerobic-responsive element (ARE); (3) hormone-responsive elements, such as ABA-responsive element (ABRE), auxin-responsive element (TGA element), salicylic acid-responsive element (TCA-element), and MeJA-responsive element (CGTCA motif/TGACG motif); (4) light-responsive elements,

such as Box 4, G-box, GT1-motif, and SP1. There were 33, 66, 184, and 182 elements responsible for plant growth and development, stress response, hormone response, and light response, respectively, accounting for 7%, 14%, 40%, and 39% of all CREs in the *HvSAD* promoter regions. *HvSADs* had the most hormone-responsive elements distributed in the promoter regions, and except for *HvSAD4*, they all contained ABRE elements.

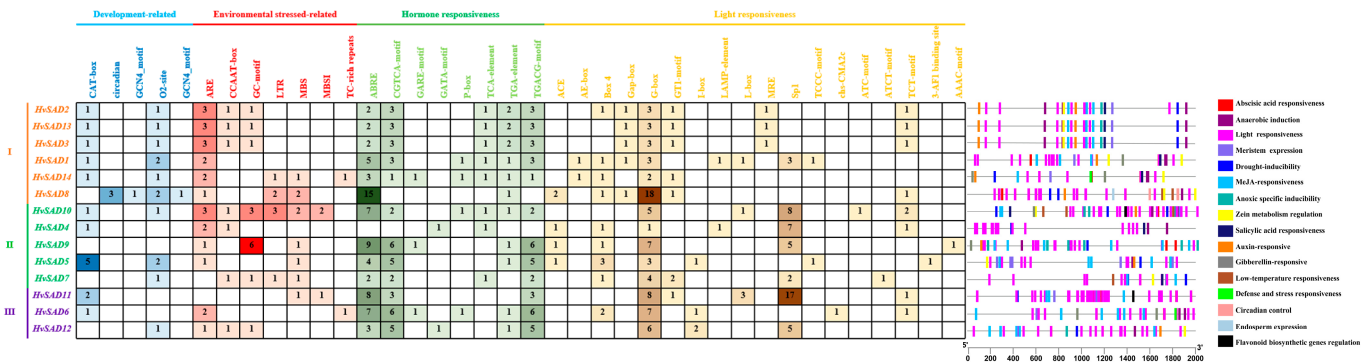


Figure 4. CREs distribution in the promoter regions of *HvSADs*. The CREs in the promoter of each *HvSAD* were classified based on the putative functions, including hormone-responsive CREs, light-responsive CREs, environmental stress-responsive CREs, and growth and development-responsive CREs. The positional distribution of various CREs on promoters is shown as rectangles with different colors. The number in each box represents the quantity of each CRE for the corresponding gene.

The element’s response to plant hormones, light, and environmental stresses was detected in all the *HvSADs*, while only growth and development regulation elements were lacking in the *HvSAD9*. In plant growth and development, the CRE related to light response and meristem expression (CAT-box, 15) was relatively high. In hormone response, the CREs associated with ABA (ABRE, 69) and MeJA (TGACG motif, 42; CGTCA motif, 42) were the most. In the stress response, the CREs related to anaerobic response (ARE, 24) and GC motif (14) were relatively high. The above results indicated that *HvSADs* are not only induced by adversity, hormones, and light, but may participate in plant growth and development processes. The different numbers of CREs reflect the different modes in which *SADs* are regulated.

2.6. Chromosome Location and Gene Duplication Analysis of *HvSADs*

HvSADs are unevenly distributed on four of the seven barley chromosomes (Figure 5). Among them, there are six, four, and three genes on chromosomes 2, 3, and 5, respectively, while only one *HvSAD* is present on chromosome 7, and most *HvSADs* are located near the ends of the chromosome arm.

Tandem and segmental duplication are two forms of gene duplication events that are major forces driving the expansion of gene families and the evolution of the entire genome [27]. Collinearity analysis revealed the presence of *SAD* gene duplication in the barley genome. Based on the evolutionary relationships and the distance between homologous gene pairs, two pairs of genes were each determined to have undergone tandem and segmented duplication (Figure 6). For instance, *HvSAD2* and *HvSAD13* underwent tandem replication and are tightly arranged on the same chromosome to form gene clusters with similar sequences and functions. In the same family, *HvSAD4* and *HvSAD9* are, respectively, located at a distance of 2H and 3H, which is the result of segmental duplication. To further explore selective pressure in barley, the synonymous (K_s) and nonsynonymous (K_a) nucleotide substitution rates of four homolog pairs were calculated (Supplementary Table S3). The K_a/K_s ratio is an important indicator reflecting the type and intensity of selection pressure during evolution, with $K_a/K_s < 1$ indicating negative selection pressure and $K_a/K_s > 1$ indicating positive selection pressure. Hence, the *HvSAD2/HvSAD13* gene pair (tandem duplication was displayed in a red box) with $K_a/K_s = 2.55$ underwent positive

selection during evolution. The Ka/Ks of the *HvSAD4/HvSAD9* gene pair (segmental duplication) is 0.08, indicating that *HvSADs* possibly underwent purifying selection.

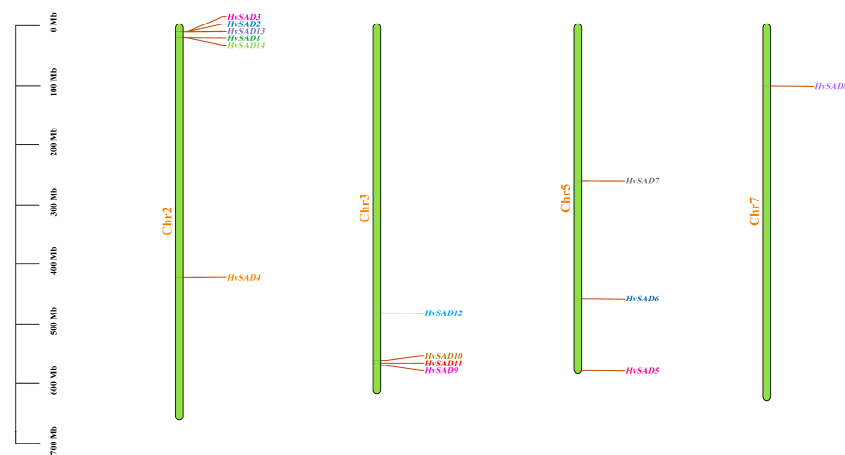


Figure 5. Chromosome distribution of *HvSADs*. Chromosome numbers are shown at the left of each chromosome, and the name of each *HvSAD* is labeled on the right side of each chromosome. The scale bar on the left side indicates the chromosome lengths (Mb).

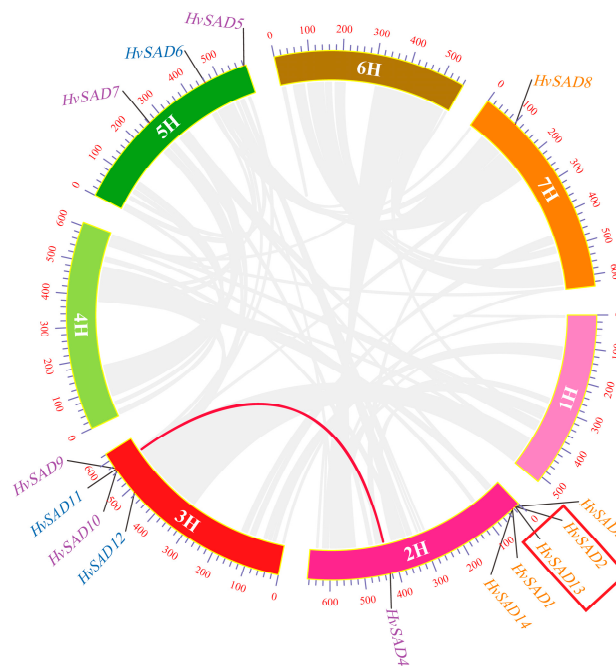


Figure 6. Gene duplications of *HvSADs*. Segmentally duplicated *HvSAD* gene pairs are linked by the red lines between chromosomes. Segmentally duplicated gene pairs within the rice genome are linked by the gray lines. The tandem duplication gene pairs are displayed in a red box. The chromosome numbers are shown at the center of each chromosome. The scale bar marked on the chromosome indicates chromosome lengths (Mb).

The syntenic relationships of *SADs* between barley and four other representative species (wheat, rice, maize, and *Brachypodium distachyon*) separately revealed 33, 6, 7, and 7 collinear gene pairs (Figure 7, Supplementary Table S5). The *SADs* have greater collinearity between barley and wheat and exhibit high homology with other monocotyledonous plants. Additionally, *HvSAD4* and *HvSAD9* exhibit multi-collinearity among species, indicating that they are more evolutionarily conserved.

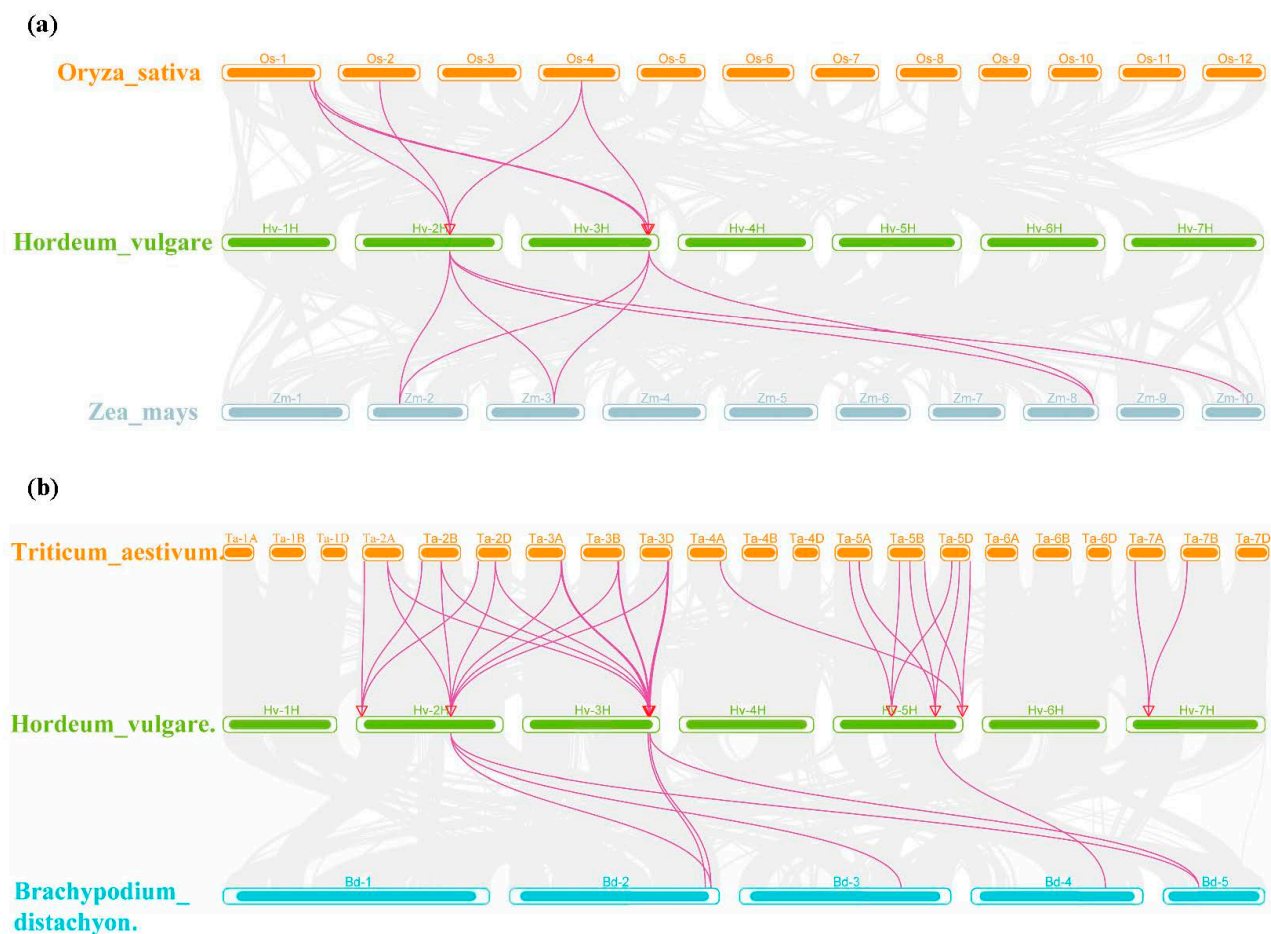


Figure 7. Collinearity relationship of the SADs in barley and four other plant species, including rice and maize (a), wheat, and *Brachypodium distachyon* (b). Gray lines in the background indicate the syntenic blocks between barley and other plant genomes, while the purple lines highlight the syntenic *HvSAD* gene pairs and red triangles show gene locations.

2.7. Expression Profiles of *HvSADs* in Different Tissues

The expression data of 16 different growth stages and tissues of barley Morex were obtained from the BARLEX website, and clustered heatmaps of 13 *HvSADs* genes (The expression data of *HvSAD2* was absent on the website) were produced using TBtools v1.116 (accessed on 28 February 2023). Different colors and circle sizes indicated different expression levels (Figure 8). The expression patterns of genes are often related to their functions, and related analysis can provide clues for potential functional studies. The results indicated that *HvSADs* mainly exhibit three expression patterns in different tissues/organs. The first type was highly expressed during the reproductive growth stage, among the expression levels of *HvSAD4*, *HvSAD6*, *HvSAD7*, *HvSAD9*, and *HvSAD10* increased from the young developing inflorescences (5 mm) (INF1) to developing inflorescences (1–1.5 cm) (INF2) stage and further increased during the grain development stage. It is speculated that *HvSADs* may also be related to barley yield. The second type of *HvSADs* was mainly expressed during the nutrient growth stage, such as *HvSAD8* and *HvSAD11*, which were highly expressed at this stage but exhibited low expression at other tissue stages. Due to their obvious tissue specificity, these genes may be necessary for spike morphogenesis. The third type of *HvSADs* was almost not expressed in any tissue, including *HvSAD3*, *HvSAD5*, *HvSAD12*, and *HvSAD13*.

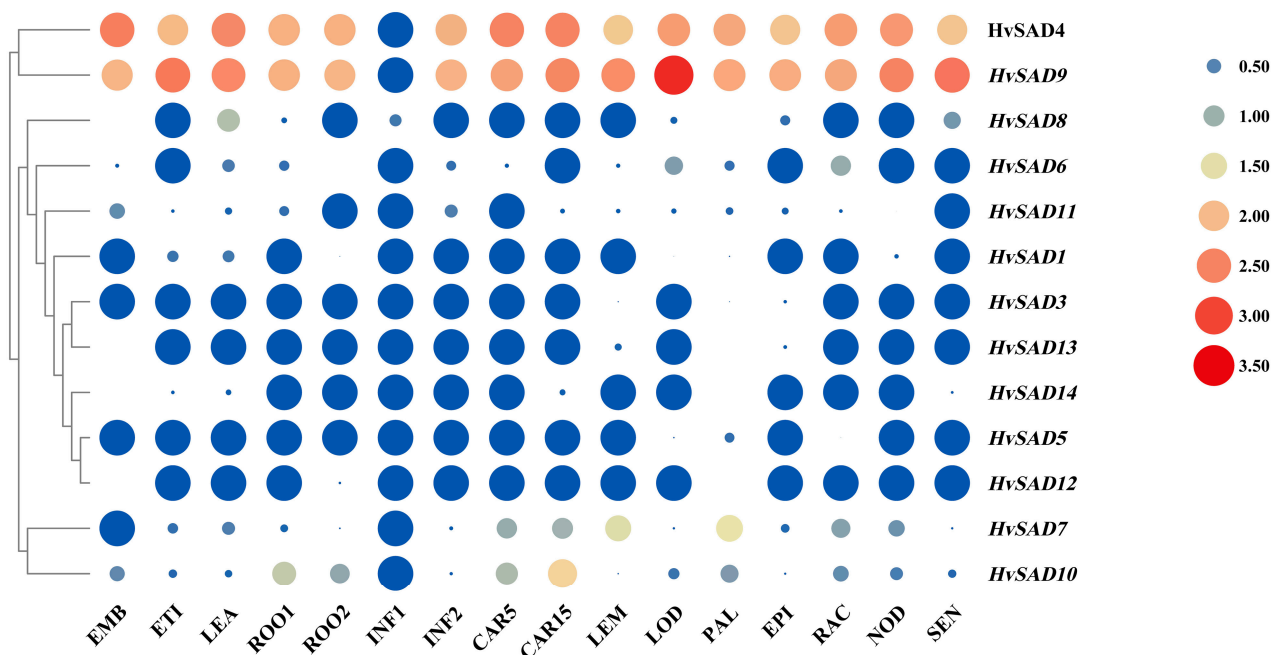


Figure 8. Expression profiles of *HvSADs* in different tissues and development stages.

Rows represent *SAD* members, while columns show different developmental stages and tissues. The expression level of *SADs* [$\log_{10}(\text{FPKM}+1)$] is shown by the intensity of color, wherein blue blocks represent low expression and red blocks represent high expression. Different-sized circles describe the value of expression level, while blue circles indicate a value of zero. EMB, 4 day embryos; ETI, etiolated seedling, dark condition (10 DAP); LEA, shoots from seedlings (10 cm shoot stage); ROO1, roots from seedlings (10 cm shoot stage); ROO2: roots (28 DAP); INF1, young developing inflorescences (5 mm); INF2, developing inflorescences (1–1.5 cm); CAR5, CAR15: developing grain (5 DAP, 15 DAP); LEM, inflorescences, lemma (42 DAP); LOD, inflorescences, lodicule (42 DAP); PAL, dissected inflorescences, palea (42 DAP); EPI, epidermal strips (28 DAP); RAC, inflorescences, rachis (35 DAP); NOD, developing tillers, 3rd internode (42 DAP); SEN, senescing leaves (56 DAP).

2.8. Expression of 10 *HvSADs* under Abiotic Stress by qRT-PCR

To investigate the potential role of *HvSADs* in abiotic stress, barley seedlings at the third leaf stage were subjected separately to salt (200 mM), drought [20% (m/V) PEG6000], and cold (4 °C) stress treatments for 0, 4, and 12 h. Ten *HvSADs* with good primer specificity were selected for investigation, and qRT-PCR was used to detect the expression of genes in seedling leaves under three stress conditions. The results showed that most *HvSADs* exhibited significantly lower expression than the control for most of the time after drought, cold, and salt treatments, whereas the expression of most *HvSADs* was significantly upregulated under salt stress (Figure 9a–c). The selected *HvSADs* exhibited differential expression over time, but their response patterns varied under different stress conditions. Among them, *HvSAD4*, *HvSAD7*, and *HvSAD9* did not respond to cold stress but showed a significant upward and downward regulation trend under drought and salt treatments. Most notably, *HvSAD11* and *HvSAD12* showed highly significant upregulation under drought and salt stress treatments but a downregulation trend under cold stress. The above findings indicate that *HvSADs* respond to abiotic stresses and may participate in the response to environmental stress.

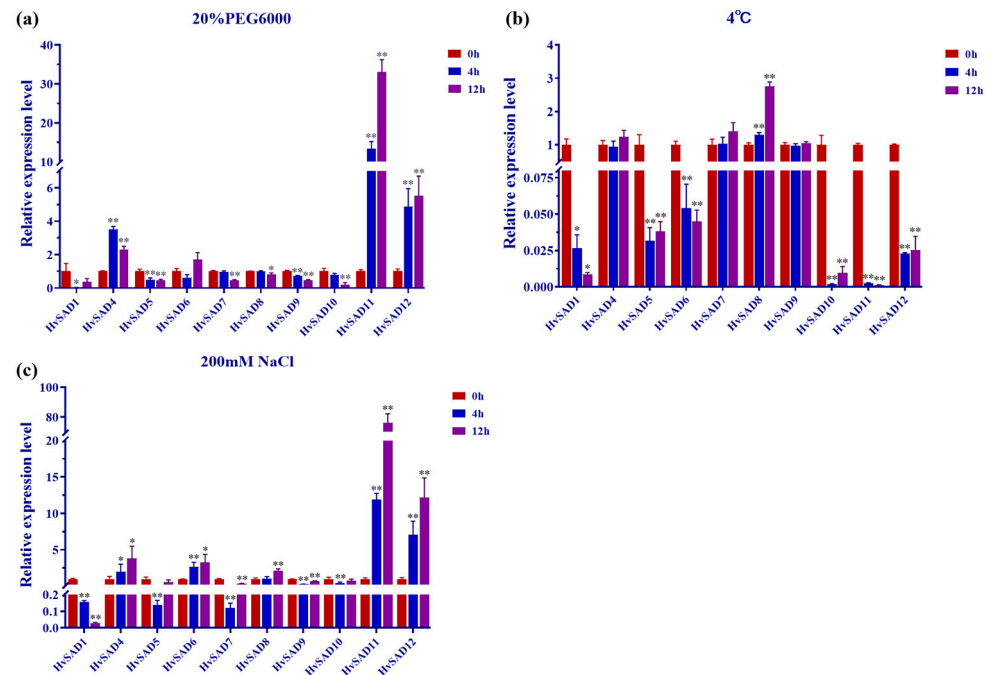


Figure 9. Expression analysis of 10 selected *HvSADs* under abiotic stresses using qRT-PCR, *viz.* drought (a), cold (b), salt (c) stresses. The *y*-axis represents the relative expression level of the *HvSAD* gene in plant leaves based on qRT-PCR analysis. The *x*-axis represents the analyzed *HvSADs*, with the red column representing a treatment time of 0 h, the blue column representing 4 h, and the purple column representing a treatment time of 12 h. A *t*-test was used to analyze significant differences in data, “*” represents $p < 0.05$, and “***” represents $p < 0.01$. Error bars represent standard deviations of the means from three technical replicates.

3. Discussion

Research on fatty acids has indicated that UFAs are essential and important nutrients for the human body. Additionally, UFAs are also an important component of plant cells, and so the study of their synthesis and functional mechanisms has important theoretical and practical significance. In plants, *SADs* have been cloned and characterized from *Arabidopsis* [28], peanut [29], cacao [8], cotton [30], and soybean [5], but there have been no reports on barley. Therefore, the identification and characterization of the *HvSADs* family at the genome-wide level will help elucidate their functional and evolutionary relationships in important crops. In this study, we comprehensively analyzed *HvSADs* and investigated their potential functions in development and abiotic stress responses.

In total, 14 *SADs* were identified in the barley genome and divided into four groups (Classes I–IV). Compared with cotton, tomato, and soybean, *SADs* from barley have a higher homology with wheat, rice, and maize, indicating that this gene family may potentially have more conservative evolution in monocotyledonous plants. The majority of *HvSADs* in the same group also showed relatively small changes in the exon–intron structure, motifs, and domain distribution, suggesting that *HvSADs* are more conserved within the species. The *SADs* in barley have relatively similar protein lengths and MWs among different groups, and it is similar in length and MW to *SAD* proteins in studied species such as *Arabidopsis* [28] and cocoa [8]. The FA_desaturase_2 domain of barley *SADs* has conserved histidine (EENRHG/DEKRHE) enriched regions [31], located in Motif2 and Motif1. Aspartic acid (D) and histidine (H) provide necessary binding sites and catalytic activity for Fe^{2+} *HvSAD* protein monomers [32]. The *HvSADs* in Group II have a higher proportion of introns compared to other members, and the retention of introns during transcription and translation may also increase compared to other members, thereby regulating gene expression and generating proteomic diversity, and even leading to phenotypic variation [33]. Interestingly, *HvSADs* (except *HvSAD12*) have chloroplast

transit peptides, and some members also have mitochondrial transit peptides, which is consistent with the predicted localization results (Supplementary Table S4). This is different from cotton and oil tea, where HvSADs are not only localized in chloroplasts but also in mitochondria [30,34]. The above implies that HvSADs play a key role in plant photosynthesis and respiration. The existence of a link between plant photorespiration metabolism and fatty acid metabolism has been reported in soybean and *Arabidopsis* [35–37].

New genes mainly originate from gene duplication. Some duplicated genes undergo functionalization, which in plants encompasses varying degrees of functional differentiation and promotes the diversity of gene functions [38–40]. Analysis of the gene duplication events indicated that some *HvSADs* underwent tandem and segmental duplication processes in a similar way as the expansion of barley *GRAS* and *Arabidopsis* gene families [27,41]. Consequently, the expansion of the barley *SAD* family may also be the result of the combined effects of tandem and segmental duplication. Tandem duplication mainly occurs in the chromosomal recombination region, implying that recombination occurred in the regions where *HvSAD2* and *HvSAD13* are located. The Ka/Ks ratio of the segmentally duplicated *HvSAD* gene pairs was less than one. They underwent a purifying selection during the evolutionary process, avoiding detrimental mutations. This is crucial for the functional protection of the *HvSAD* family [42] (Supplementary Table S3). The collinearity analysis among different species showed that *HvSADs* have a high homology with Gramineae plants, especially wheat. *HvSAD4* and *HvSAD9* displayed multiple collinearities among species, providing potential clues for the origin and evolution of *HvSADs*. The conservation and functional diversity exhibited by the gene family during evolution enhances the adaptability of plants to various unfavorable survival environments, such as drought, disease, and temperature extremes, to ensure their growth and development [43,44].

The CREs themselves do not encode any proteins but typically bind to transcription factors to regulate the expression of adjacent genes. During plant growth, differentiation, and development, it is necessary to integrate signals from different tissues, development, and environments to regulate gene expression. Therefore, it is extremely important to focus on specific elements that regulate transcription initiation [45]. In the promoter regions, we identified a large number of CREs associated with hormone response, light response, and stress response, as well as a few growth and development elements. The number of light-responsive elements was the highest (182), followed by MeJA elements (CGTCAMotif/TGACG Motif, 84) and ABA reaction elements (ABRE, 69). It has been found that *Chlorella* significantly upregulated the transcription of *SAD* to induce the accumulation of total fatty acids, including oleic acid, under high light stress [46]. However, olives treated under dark conditions showed a significant 90-fold reduction in the level of *SAD1* and *SAD3* transcripts, but no noticeable difference in the total UFA content [47]. Hormones are also essential in regulating plant growth and development. MaABI5-like regulated ABA-induced cold tolerance by increasing the content of UFAs and flavonoids [48]. In *Arabidopsis*, the level of linolenic acid was increased through exogenous MeJA treatment to enhance drought and salt tolerance as well as cold tolerance [49]. Furthermore, MeJA participates in plant signal transduction, induces the synthesis of defensive compounds, and plays a great part in plant resistance to stresses and diseases [44,50]. The above results emphasize that utilizing CREs that potentially affect plant development and environmental response can be used to promote crop improvement.

In some plants, *SADs* have been found to have tissue and stage-specific expression. *AhSAD3* in peanuts was mainly expressed in developing seeds in accordance with the oil accumulation stage, while *AhSAD1/2* was expressed in developing seeds, leaves, stems, roots, and flowers, and the expression level in the flowers was even higher than that in the seeds [29]. In *Arabidopsis*, the double mutations in both *FAB2* and *AAD5*, two *SAD*-encoding genes, caused embryo development to stop before the globular stage, and these two genes along with *AAD1*, another *SAD*-encoding gene, participated in the formation of embryonic keratin in the later stage of seed growth [7]. *OeSAD1* was expressed most highly in olive leaves and least in the flowers, while *OeSAD2* was mainly expressed in the fruit peel and

was lowest in the leaves, exhibiting a significant inducing effect in the fruit [51]. This study showed that *HvSADs* are not only expressed in a specific tissue type. For example, *HvSAD4* and *HvSAD9* were expressed at higher levels in each tissue compared to other members, suggesting that they have a regulatory effect on multiple development stages. However, *HvSADs* also exhibited high expression levels in specific tissue types, such as *HvSAD10* being most expressed in CAR15, which is consistent with the research results in peanuts.

Existing studies have shown that *SADs* are associated with plant abiotic stress resistance, particularly with a crucial impact on cold stress resistance [10,47,52–55]. In tea trees and flax, the expression of the *SADs* was strongly induced by cold and drought stresses [52,55]. It is noteworthy that in addition to most ARE and GC motifs, the *HvSADs* also had CCAAT-box (MYBHv1 binding site), MBS (MYB binding site involved in drought-inducibility), LTR (low-temperature responsiveness), TC-rich repeats (defense and stress responsiveness), and MBSI (MYB binding site involved in the regulation of flavonoid biosynthesis genes) elements, which offer the possibility of the *HvSADs* to respond promptly to drought, cold, and salt stresses. [56,57] In the study, *HvSADs* were also found to respond to cold, drought, and salt stresses, but each member responded to different stresses in different ways. Low-temperature stress often leads to the fixation of membrane proteins, and the content of UFAs in plants increases to a certain extent in order to maintain the fluidity of the cell membrane [47]. *HvSAD8* was significantly upregulated by cold stress, with the highest expression level in the aboveground parts of the seedlings, implying that it is important for the protection of barley seedlings against severe cold. The expression levels of *HvSAD5* and *HvSAD10* were significantly downregulated and then upregulated under cold stress, indicating a rapid response to stress and controlled through negative regulation. In addition to positively responding to cold stress, studies have also found that increasing the content of UFAs in plant membrane lipids can greatly enhance the tolerance of the photosynthetic machinery to salt stress. In *Arabidopsis*, salt stress significantly reduced the expression of *AtACP5*, and knocking out the gene increased the sensitivity of plants to salt stress. The overexpression of *AtACP5* led to changes in FA composition, thereby improving salt tolerance [58,59]. Similar to other abiotic stresses, plants resist drought stress by regulating the content of UFAs [60,61]. *HvSAD11* and *HvSAD12* strongly responded to drought and salt stress and were significantly upregulated after 4 h and 12 h, exhibiting greater upregulation under these stresses compared to cold stress. This may be related to the fact that, compared to other cereal crops, barley itself has strong salt, drought, and cold tolerance. The *SAD* family in plants influences lipid synthesis, seed development, and stress resistance, which has positive implications for genetic improvement and breeding in plants [53,62,63].

4. Materials and Methods

4.1. Identification of *SADs* in Barley

To find candidate *SADs* in the barley genome, the hidden Markov model profile of the PF03405 (FA_desaturase_2 domain) file was downloaded from the Pfam database (<http://pfam-legacy.xfam.org/>) (accessed on 24 August 2022) [64,65], and the protein sequences with this domain were screened using TBtools v1.098669 (accessed on 24 August 2022) (E-value $\leq 10^{-5}$) [66]. Meanwhile, for reliable results, the identified sequences of seven *SADs* of *Arabidopsis* were also used as reference sequences, and a BLASTP search was performed with the barley genome in the Ensembl Plants database (<http://plants.ensembl.org/index.html>) (accessed on 24 August 2022) as well as in the BARLEX database (<http://barlex.barleysequence.org>) (accessed on 24 August 2022), with an E-value $\leq 10^{-5}$ and identity $\geq 50\%$ set as the filtering conditions to obtain the potential *HvSAD* members [28,67,68]. Using NCBI (<https://www.ncbi.nlm.nih.gov>) (accessed on 25 August 2022) and SMART (<http://smart.embl-heidelberg.de/>) (accessed on 25 August 2022) online software, domain validation was performed on the screened barley *SAD* protein sequences [69]. Next, the incomplete reading frame and short and redundant sequences were removed manually, after which the *SAD* gene and protein sequences in barley were finally obtained.

4.2. Physicochemical Properties Analysis

The composition and physical and chemical characteristics of the HvSADs were analyzed with ExPASy (<https://web.expasy.org/>) (accessed on 1 September 2022), and the sub-cellular localizations of the HvSADs were assessed using WoLF PSORT (<https://wolfpsort.hgc.jp/>) (accessed on 1 September 2022) [70,71]. Signal and chloroplast transit peptides were predicted using Ipsort (<https://ipsort.hgc.jp/>) (accessed on 1 September 2022) [72]. Detailed information on all HvSADs is provided in Table 1.

4.3. Phylogenetic Analysis

A phylogenetic tree of SADs among eight plant species was constructed using the neighbor-joining (NJ) method in MEGA7.0 software. The bootstrap value was set to 1000, and Evolview (<http://www.evolgenius.info/evolview/#/>) (accessed on 7 March 2023) was used to display the evolutionary tree [73,74]. Additionally, to study the characteristic structural domains of barley SAD members, multiple sequence comparisons of HvSAD protein sequences were performed using DNAMAN version: 9.0.1.116 (accessed on 7 March 2023).

4.4. Analysis of Conserved Motif and Gene Structure

The exon-intron structures of HvSADs were examined using TBtools and the GFF3 data (Generic Feature Format version 3 Data) from Ensembl Plants. The conserved motifs of HvSADs performed a thorough investigation with MEME (<http://meme-suite.org/>) (accessed on 12 February 2023), with a maximum of 10 motifs and motif width between 6 and 50 amino acid residues. Finally, the full graphics of the conserved motif and gene structure were visualized by the BioSequence Structure Drawers function of TBtools.

4.5. Cis-Regulatory Elements Prediction in the Promoter Regions of HvSADs

For each HvSAD, a 2000 bp sequence upstream of the initiation codon (ATG) was extracted using TBtools v1.116 (accessed on 12 February 2023) and submitted to the PlantCARE website (<http://bioinformatics.psb.ugent.be/webtools/plantcare/html/>) (accessed on 12 February 2023) to obtain information on CREs [75]. The obtained prediction information was categorized and summarized. Eventually, the CREs were displayed using TBtools and Excel 2016 software (Microsoft Corp., Redmond, WA, USA).

4.6. Chromosome Distribution, Gene Duplication, and Selective Pressure Analysis

Genomic data of barley, wheat (*Triticum aestivum*), rice (*Oryza sativa*), maize (*Zea mays*), and *Brachypodium distachyon* were downloaded from the Ensembl Plants database. The TBtools v1.116 (accessed on 9 February 2023) was used to analyze and visualize the chromosomal distribution, gene duplication events within the barley genome, as well as the gene level collinearity among plant genomes. The Simple Ka/Ks Calculator (NG) tool in TBtools v1.116 (accessed on 9 August 2023) was used to calculate the ratio of non-synonymous to synonymous substitution (Ka/Ks) for duplicated gene pairs.

4.7. Expression Analysis of HvSADs Members

The expression levels of HvSADs in different tissues and development stages were downloaded from the transcriptome data of RNA sequence from the BARLEX database. The gene expression values are represented by fragments per kilobase of exon per million fragments mapped (FPKM). A heatmap of the expression pattern was analyzed by TBtools to analyze the expression of each SAD in different tissues of barley.

4.8. Plant Material, Stress Treatment, RNA Extraction, and qRT-PCR Analysis

After disinfecting the barley Morex seeds, they were germinated under dark conditions at 24 °C. Seedlings exhibiting strong and consistent growth were selected for hydroponic cultivation and were cultivated with 1/2 Hoagland's nutrient solution in an artificial illumination incubator under a day/night temperature of 24 °C/22 °C with 14 h of 100% of

full light and 10 h of darkness. The nutrient solution was changed every three days. At the third-leaf stage, the seedlings were treated under low-temperature stress (4 °C), salt stress (200 mM NaCl), and simulated drought stress [20% polyethylene glycol (PEG)6000] separately. The control group was cultivated with a nutrient solution only. The leaves were, respectively, sampled at 0 h, 4 h, and 12 h and stored at −80 °C after rapidly freezing with liquid nitrogen.

Total RNA was extracted using a Plant RNA Extraction Kit (Promega, Beijing, China) and then reversely transcribed to cDNA by a Reverse Transcription Kit (YEASEN, Shanghai, China), all according to the reagent instructions. The quantitative real-time PCR (qRT-PCR) amplification was performed using Hieff® qPCR SYBR Green Master Mix (YEASEN, Shanghai, China) in a CFX96 Touch™ Real-Time PCR Detection System (Bio-Rad, Hercules, CA, USA). Primers were designed according to the CDS sequences of *HvSADs* using Primer Premier 5 software (Premier Biosoft Interpairs, Palo Alto, CA, USA) with the following settings: PCR product size for 100–300 bp, primer length for 22 ± 3 bp. Their specificity was then confirmed by using the Ensembl Plants database for BLASTN search in the barley genome. *HvActin* (*HORVU. MoreX.r3.1HG0003140*) was used as the internal reference gene. The sequence information of all primers is listed in Supplementary Table S1. Three biological replicates and three technical replicates were tested for each sample, and the relative expression levels were calculated using the $2^{-\Delta\Delta C_t}$ method [76]. Gene expressions for selected *HvSADs* were analyzed using GraphPad Prism version 9.5.0 for Windows (GraphPad Software, San Diego, California USA, www.graphpad.com).

5. Conclusions

This study identified 14 *HvSADs* genes from the barley genome. Based on a phylogenetic and gene structure analysis, the *HvSADs* were classified as Class I to Class IV. Members of the same group exhibited similar structural characteristics. Gene replication analysis indicated that tandem duplication, fragment duplication, and purification selection contributed to the expansion and evolution of the *HvSAD* family. In addition, a commonality analysis between barley, rice, wheat, maize, and *Brachypodium distachyon* showed varying degrees of correlation. The *HvSADs* were found to be influenced by various factors, including hormones, light, and stress. In addition, the *HvSADs* were highly expressed during young ear and seed development and may be involved in the regulation of reproductive growth. Several *HvSADs* exhibited different expression patterns under abiotic stress. Overall, the genome-wide identification and molecular characterization of *HvSADs* provide new insights into their evolutionary history and functional roles, contributing to a comprehensive analysis of the regulatory mechanisms and genetic improvement of plant oil biosynthesis and metabolism.

Supplementary Materials: The following supporting information can be downloaded at: <https://www.mdpi.com/article/10.3390/ijms25010113/s1>.

Author Contributions: Conceptualization, X.Z. (Xiaoqin Zhang), Y.F. and D.X.; Methodology, M.D., D.Z., X.Z. (Xian Zhang), Q.T. and W.M.; Investigation, M.D., Y.Y., S.W. and C.D.; writing—review & editing, D.X. All authors have read and agreed to the published version of the manuscript.

Funding: This research was funded by Hangzhou Normal University Graduate Research Innovation Promotion Project (grant number: 2022HSDYJSKY223). And The APC was funded by Hanzhou Normal University.

Institutional Review Board Statement: Not applicable.

Informed Consent Statement: Not applicable.

Data Availability Statement: Data is contained within the article and supplementary materials.

Conflicts of Interest: The authors declare no conflict of interest.

References

- McKeon, T.A.; Stumpf, P.K. Purification and Characterization of the Stearoyl-Acyl Carrier Protein Desaturase and the Acyl-Acyl Carrier Protein Thioesterase from Maturing Seeds of Safflower. *J. Biol. Chem.* **1982**, *257*, 12141–12147. [[CrossRef](#)] [[PubMed](#)]
- Fox, B.G. Stearoyl-Acyl Carrier Protein $\Delta 9$ Desaturase from *Ricinus Communis* Is a Diiron-Oxo Protein. *Proc. Natl. Acad. Sci. USA* **1993**, *90*, 2486–2490. [[CrossRef](#)] [[PubMed](#)]
- Han, Y.; Xu, G.; Du, H.; Hu, J.; Liu, Z.; Li, H.; Li, J.; Yang, X. Natural Variations in Stearoyl-Acp Desaturase Genes Affect the Conversion of Stearic to Oleic Acid in Maize Kernel. *Theor. Appl. Genet.* **2017**, *130*, 151–161. [[CrossRef](#)]
- Ohlrogge, J.; Browse, J. Lipid Biosynthesis. *Plant Cell* **1995**, *7*, 957–970. [[CrossRef](#)] [[PubMed](#)]
- Deng, M.; Liu, B.; Wang, Z.; Xue, J.; Zhang, H.; Li, R. Identification and Functional Analysis of Soybean Stearoyl-ACP $\Delta 9$ Desaturase (GmSAD) Gene Family. *Sheng Wu Gong Cheng Xue Bao* **2020**, *36*, 716–731. [[CrossRef](#)] [[PubMed](#)]
- Liu, B.; Sun, Y.; Xue, J.; Mao, X.; Jia, X.; Li, R. Stearoyl-ACP $\Delta 9$ Desaturase 6 and 8 (GhA-SAD6 and GhD-SAD8) Are Responsible for Biosynthesis of Palmitoleic Acid Specifically in Developing Endosperm of Upland Cotton Seeds. *Front. Plant Sci.* **2019**, *10*, 703. [[CrossRef](#)] [[PubMed](#)]
- Kazaz, S.; Barthole, G.; Domergue, F.; Ettaki, H.; To, A.; Vasselon, D.; De Vos, D.; Belcram, K.; Lepiniec, L.; Baud, S. Differential Activation of Partially Redundant $\Delta 9$ Stearoyl-ACP Desaturase Genes Is Critical for Omega-9 Monounsaturated Fatty Acid Biosynthesis During Seed Development in *Arabidopsis*. *Plant Cell* **2020**, *32*, 3613–3637. [[CrossRef](#)]
- Zhang, Y.; Maximova, S.N.; Guiltinan, M.J. Characterization of a Stearoyl-Acyl Carrier Protein Desaturase Gene Family from Chocolate Tree, *Theobroma cacao* L. *Front. Plant Sci.* **2015**, *6*, 239. [[CrossRef](#)]
- Tasseva, G.; Davy De Virville, J.; Cantrel, C.; Moreau, F.; Zachowski, A. Changes in the Endoplasmic Reticulum Lipid Properties in Response to Low Temperature in *Brassica napus*. *Plant Physiol. Biochem.* **2004**, *42*, 811–822. [[CrossRef](#)]
- Li, F.; Bian, C.S.; Xu, J.F.; Pang, W.F.; Liu, J.; Duan, S.G.; Lei, Z.-G.; Jiwan, P.; Jin, L.-P. Cloning and Functional Characterization of SAD Genes in Potato. *PLoS ONE* **2015**, *10*, e0122036. [[CrossRef](#)]
- Byfield, G.E.; Upchurch, R.G. Effect of Temperature on Delta-9 Stearoyl-ACP and Microsomal Omega-6 Desaturase Gene Expression and Fatty Acid Content in Developing Soybean Seeds. *Crop Sci.* **2007**, *47*, 1698–1704. [[CrossRef](#)]
- Sui, N.; Li, M.; Li, K.; Song, J.; Wang, B.S. Increase in Unsaturated Fatty Acids in Membrane Lipids of *Suaeda salsa* L. Enhances Protection of Photosystem II under High Salinity. *Photosynthetica* **2010**, *48*, 623–629. [[CrossRef](#)]
- Sui, N.; Tian, S.; Wang, W.; Wang, M.; Fan, H. Overexpression of Glycerol-3-Phosphate Acyltransferase from *Suaeda salsa* Improves Salt Tolerance in *Arabidopsis*. *Front. Plant Sci.* **2017**, *8*, 1337. [[CrossRef](#)] [[PubMed](#)]
- Sui, N.; Wang, Y.; Liu, S.; Yang, Z.; Wang, F.; Wan, S. Transcriptomic and Physiological Evidence for the Relationship between Unsaturated Fatty Acid and Salt Stress in Peanut. *Front. Plant Sci.* **2018**, *9*, 7. [[CrossRef](#)]
- Mo, S.; Zhang, Y.; Wang, X.; Yang, J.; Sun, Z.; Zhang, D.; Chen, B.; Wang, G.; Ke, H.; Liu, Z.; et al. Cotton GhSSI2 Isoforms from the Stearoyl Acyl Carrier Protein Fatty Acid Desaturase Family Regulate Verticillium Wilt Resistance. *Mol. Plant Pathol.* **2021**, *22*, 1041–1056. [[CrossRef](#)] [[PubMed](#)]
- Sharma, P.; Jha, A.B.; Dubey, R.S.; Pessarakli, M. Reactive Oxygen Species, Oxidative Damage, and Antioxidative Defense Mechanism in Plants under Stressful Conditions. *J. Exp. Bot.* **2012**, *2012*, 217037. [[CrossRef](#)]
- Farmer, E.E.; Mueller, M.J. ROS-Mediated Lipid Peroxidation and RES-Activated Signaling. *Annu. Rev. Plant Biol.* **2013**, *64*, 429–450. [[CrossRef](#)] [[PubMed](#)]
- Choudhary, A.; Kumar, A.; Kaur, N. ROS and Oxidative Burst: Roots in Plant Development. *Plant Divers.* **2020**, *42*, 33–43. [[CrossRef](#)]
- Giraldo, P.; Benavente, E.; Manzano-Agugliaro, F.; Gimenez, E. Worldwide Research Trends on Wheat and Barley: A Bibliometric Comparative Analysis. *Agronomy* **2019**, *9*, 352. [[CrossRef](#)]
- Zhang, L.; Wang, S.; Chen, Y.; Dong, M.; Fang, Y.; Zhang, X.; Tong, T.; Zhang, Z.; Zheng, J.; Xue, D.; et al. Genome-Wide Identification of the F-Box Gene Family and Expression Analysis under Drought and Salt Stress in Barley. *Phyton* **2020**, *89*, 229–251. [[CrossRef](#)]
- Zhang, Z.; Tong, T.; Fang, Y.; Zheng, J.; Zhang, X.; Niu, C.; Li, J.; Zhang, X.; Xue, D. Genome-Wide Identification of Barley ABC Genes and Their Expression in Response to Abiotic Stress Treatment. *Plants* **2020**, *9*, 1281. [[CrossRef](#)] [[PubMed](#)]
- Zhang, X.; Zhang, L.; Chen, Y.; Wang, S.; Fang, Y.; Zhang, X.; Wu, Y.; Xue, D. Genome-Wide Identification of the SOD Gene Family and Expression Analysis under Drought and Salt Stress in Barley. *Plant Growth Regul.* **2021**, *94*, 49–60. [[CrossRef](#)]
- Zhang, C.; Yang, Q.; Zhang, X.; Zhang, X.; Yu, T.; Wu, Y.; Fang, Y.; Xue, D. Genome-Wide Identification of the HMA Gene Family and Expression Analysis under Cd Stress in Barley. *Plants* **2021**, *10*, 1849. [[CrossRef](#)] [[PubMed](#)]
- Tong, T.; Fang, Y.; Zhang, Z.; Zheng, J.; Lu, X.; Zhang, X.; Xue, D. Genome-Wide Identification, Phylogenetic and Expression Analysis of SBP-Box Gene Family in Barley (*Hordeum vulgare* L.). *Plant Growth Regul.* **2020**, *90*, 137–149. [[CrossRef](#)]
- Tong, T.; Fang, Y.; Zhang, Z.; Zheng, J.; Zhang, X.; Li, J.; Niu, C.; Xue, D.; Zhang, X. Genome-Wide Identification and Expression Pattern Analysis of the KCS Gene Family in Barley. *Plant Growth Regul.* **2021**, *93*, 89–103. [[CrossRef](#)]
- Zheng, J.; Zhang, Z.; Tong, T.; Fang, Y.; Zhang, X.; Niu, C.; Li, J.; Wu, Y.; Xue, D.; Zhang, X. Genome-Wide Identification of WRKY Gene Family and Expression Analysis under Abiotic Stress in Barley. *Agronomy* **2021**, *11*, 521. [[CrossRef](#)]
- Cannon, S.B.; Mitra, A.; Baumgarten, A.; Young, N.D.; May, G. The Roles of Segmental and Tandem Gene Duplication in the Evolution of Large Gene Families in *Arabidopsis thaliana*. *BMC Plant Biol.* **2004**, *4*, 10. [[CrossRef](#)] [[PubMed](#)]

28. Kachroo, A.; Shanklin, J.; Whittle, E.; Lapchyk, L.; Hildebrand, D.; Kachroo, P. The Arabidopsis Stearoyl-Acyl Carrier Protein-Desaturase Family and the Contribution of Leaf Isoforms to Oleic Acid Synthesis. *Plant Mol. Biol.* **2006**, *63*, 257–271. [[CrossRef](#)]
29. Shilman, F.; Brand, Y.; Brand, A.; Hedvat, I.; Hovav, R. Identification and Molecular Characterization of Homeologous Δ^9 -Stearoyl Acyl Carrier Protein Desaturase 3 Genes from the Allotetraploid Peanut (*Arachis hypogaea*). *Plant Mol. Biol. Rep.* **2011**, *29*, 232–241. [[CrossRef](#)]
30. Shang, X.; Cheng, C.; Ding, J.; Guo, W. Identification of Candidate Genes from the SAD Gene Family in Cotton for Determination of Cottonseed Oil Composition. *Mol. Genet. Genom.* **2017**, *292*, 173–186. [[CrossRef](#)]
31. Sperling, P.; Ternes, P.; Zank, T.K.; Heinz, E. The Evolution of Desaturases. *Prostag. Leukotr. Ess.* **2003**, *68*, 73–95. [[CrossRef](#)] [[PubMed](#)]
32. Guy, J.E.; Whittle, E.; Moche, M.; Lengqvist, J.; Lindqvist, Y.; Shanklin, J. Remote Control of Regioselectivity in Acyl-Acyl Carrier Protein-Desaturases. *Proc. Natl. Acad. Sci. USA* **2011**, *108*, 16594–16599. [[CrossRef](#)] [[PubMed](#)]
33. Rocchi, V.; Janni, M.; Bellincampi, D.; Giardina, T.; D'Ovidio, R. Intron Retention Regulates the Expression of Pectin Methyl Esterase Inhibitor (Pmei) Genes during Wheat Growth and Development: Isolation and Functional Characterisation of Wheat Pmei Genes. *Plant Biol.* **2012**, *14*, 365–373. [[CrossRef](#)] [[PubMed](#)]
34. Yang, J.; Chen, B.; Manan, S.; Li, P.; Liu, C.; She, G.; Zhao, S.; Zhao, J. Critical Metabolic Pathways and SAD/FADs, WRI1s, and DGATs Cooperate for High-Oleic Acid Oil Production in Developing Oil Tea (*Camellia oleifera*) Seeds. *Hort. Res.* **2022**, *9*, uhac087. [[CrossRef](#)] [[PubMed](#)]
35. Song, G.; Li, X.; Munir, R.; Khan, A.R.; Azhar, W.; Yasin, M.U.; Jiang, Q.; Bancroft, I.; Gan, Y. The WRKY6 Transcription Factor Affects Seed Oil Accumulation and Alters Fatty Acid Compositions in *Arabidopsis thaliana*. *Physiol. Plant* **2020**, *169*, 612–624. [[CrossRef](#)] [[PubMed](#)]
36. Wang, X. Transcriptomic Analysis Reveals the Regulatory Networks and Hub Genes Controlling the Unsaturated Fatty Acid Contents of Developing Seed in Soybean. *Front. Plant Sci.* **2022**, *13*, 876371. [[CrossRef](#)]
37. Xi, Y.; Cai, J.; Li, G.; Huang, H.; Peng, X.; Zhu, G. High CO₂ Facilitates Fatty Acid Biosynthesis and Mitigates Cellular Oxidative Stress Caused by CAC2 Dysfunction in *Arabidopsis*. *Plant J.* **2023**, *115*, 1316–1330. [[CrossRef](#)]
38. Panchy, N.; Lehti-Shiu, M.; Shiu, S.-H. Evolution of Gene Duplication in Plants. *Plant Physiol.* **2016**, *171*, 2294–2316. [[CrossRef](#)]
39. Ezoë, A.; Shirai, K.; Hanada, K. Degree of Functional Divergence in Duplicates Is Associated with Distinct Roles in Plant Evolution. *Mol. Biol. Evol.* **2021**, *38*, 1447–1459. [[CrossRef](#)]
40. Jia, Y.; Xu, M.; Hu, H.; Chapman, B.; Watt, C.; Buerte, B.; Han, N.; Zhu, M.; Bian, H.; Li, C.; et al. Comparative Gene Retention Analysis in Barley, Wild Emmer, and Bread Wheat Pangenome Lines Reveals Factors Affecting Gene Retention Following Gene Duplication. *BMC Biol.* **2023**, *21*, 25. [[CrossRef](#)]
41. To, V.-T.; Shi, Q.; Zhang, Y.; Shi, J.; Shen, C.; Zhang, D.; Cai, W. Genome-Wide Analysis of the GRAS Gene Family in Barley (*Hordeum vulgare* L.). *Genes* **2020**, *11*, 553. [[CrossRef](#)] [[PubMed](#)]
42. Cvijovic, I.; Good, B.H.; Desai, M.M. The Effect of Strong Purifying Selection on Genetic Diversity. *Genetics* **2018**, *209*, 1235–1278. [[CrossRef](#)] [[PubMed](#)]
43. Nandi, A. Arabidopsis *Sfd* Mutants Affect Plastidic Lipid Composition and Suppress Dwarfing, Cell Death, and the Enhanced Disease Resistance Phenotypes Resulting from the Deficiency of a Fatty Acid Desaturase. *Plant Cell* **2003**, *15*, 2383–2398. [[CrossRef](#)] [[PubMed](#)]
44. Wasternack, C. Jasmonates: An Update on Biosynthesis, Signal Transduction and Action in Plant Stress Response, Growth and Development. *Ann. Bot.* **2007**, *100*, 681–697. [[CrossRef](#)] [[PubMed](#)]
45. Marand, A.P.; Eveland, A.L.; Kaufmann, K.; Springer, N.M. Cis-Regulatory Elements in Plant Development, Adaptation, and Evolution. *Annu. Rev. Plant Biol.* **2023**, *74*, 111–137. [[CrossRef](#)] [[PubMed](#)]
46. Liu, J.; Sun, Z.; Zhong, Y.; Huang, J.; Hu, Q.; Chen, F. Stearoyl-Acyl Carrier Protein Desaturase Gene from the Oleaginous Microalga *Chlorella Zofingiensis*: Cloning, Characterization and Transcriptional Analysis. *Planta* **2012**, *236*, 1665–1676. [[CrossRef](#)] [[PubMed](#)]
47. Hernández, M.L.; Sicardo, M.D.; Alfonso, M.; Martínez-Rivas, J.M. Transcriptional Regulation of Stearoyl-Acyl Carrier Protein Desaturase Genes in Response to Abiotic Stresses Leads to Changes in the Unsaturated Fatty Acids Composition of Olive Mesocarp. *Front. Plant Sci.* **2019**, *10*, 251. [[CrossRef](#)]
48. Song, Z.; Lai, X.; Chen, H.; Wang, L.; Pang, X.; Hao, Y.; Lu, W.; Chen, W.; Zhu, X.; Li, X. Role of MaABI5-like in Abscisic Acid-Induced Cold Tolerance of 'Fenjiao' Banana Fruit. *Hortic. Res.* **2022**, *9*, uhac130. [[CrossRef](#)]
49. Cao, J.; Li, M.; Chen, J.; Liu, P.; Li, Z. Effects of MeJA on *Arabidopsis* Metabolome under Endogenous JA Deficiency. *Sci. Rep.* **2016**, *6*, 37674. [[CrossRef](#)]
50. Yu, X.; Zhang, W.; Zhang, Y.; Zhang, X.; Lang, D.; Zhang, X. The Roles of Methyl Jasmonate to Stress in Plants. *Funct. Plant Biol.* **2019**, *46*, 197. [[CrossRef](#)]
51. Contreras, C.; Mariotti, R.; Mousavi, S.; Baldoni, L.; Guerrero, C.; Roka, L.; Cultrera, N.; Pierantozzi, P.; Maestri, D.; Gentili, L.; et al. Characterization and Validation of Olive FAD and SAD Gene Families: Expression Analysis in Different Tissues and during Fruit Development. *Mol. Biol. Rep.* **2020**, *47*, 4345–4355. [[CrossRef](#)]
52. Ding, Z.T.; Shen, J.Z.; Pan, L.L.; Wang, Y.U.; Li, Y.S.; Wang, Y.; Sun, H.W. CsSAD: A Fatty Acid Desaturase Gene Involved in Abiotic Resistance in *Camellia sinensis* (L.). *Genet. Mol. Res.* **2016**, *15*, 15017512. [[CrossRef](#)] [[PubMed](#)]
53. He, M.; Ding, N.-Z. Plant Unsaturated Fatty Acids: Multiple Roles in Stress Response. *Front. Plant Sci.* **2020**, *11*, 562785. [[CrossRef](#)] [[PubMed](#)]

54. Chen, J.; Gao, J.; Zhang, L.; Zhang, L. Tung Tree Stearoyl-acyl Carrier Protein $\Delta 9$ Desaturase Improves Oil Content and Cold Resistance of *Arabidopsis* and *Saccharomyces cerevisiae*. *Front. Plant Sci.* **2023**, *14*, 1144853. [[CrossRef](#)] [[PubMed](#)]
55. Wang, J.; Shao, Y.; Yang, X.; Zhang, C.; Guo, Y.; Liu, Z.; Chen, M. Heterogeneous Expression of Stearoyl-Acyl Carrier Protein Desaturase Genes SAD1 and SAD2 from *Linum usitatissimum* Enhances Seed Oleic Acid Accumulation and Seedling Cold and Drought Tolerance Capability in *Brassica napus*. *J. Integr. Agric.* **2023**, S2095311923001387. [[CrossRef](#)]
56. Alexander, R.D.; Wendelboe-Nelson, C.; Morris, P.C. The Barley Transcription Factor HvMYB1 Is a Positive Regulator of Drought Tolerance. *Plant Physiol. Biochem.* **2019**, *142*, 246–253. [[CrossRef](#)] [[PubMed](#)]
57. Lee, T.G.; Jang, C.S.; Kim, J.Y.; Kim, D.S.; Park, J.H.; Kim, D.Y.; Seo, Y.W. A Myb Transcription Factor (*TaMyb1*) from Wheat Roots Is Expressed during Hypoxia: Roles in Response to the Oxygen Concentration in Root Environment and Abiotic Stresses. *Physiol. Plant* **2007**, *129*, 375–385. [[CrossRef](#)]
58. Allakhverdiev, S.I.; Kinoshita, M.; Inaba, M.; Suzuki, I.; Murata, N. Unsaturated Fatty Acids in Membrane Lipids Protect the Photosynthetic Machinery against Salt-Induced Damage in *Synechococcus*. *Plant Physiol.* **2001**, *125*, 1842–1853. [[CrossRef](#)]
59. Huang, J.; Xue, C.; Wang, H.; Wang, L.; Schmidt, W.; Shen, R.; Lan, P. Genes of ACYL CARRIER PROTEIN Family Show Different Expression Profiles and Overexpression of ACYL CARRIER PROTEIN 5 Modulates Fatty Acid Composition and Enhances Salt Stress Tolerance in *Arabidopsis*. *Front. Plant Sci.* **2017**, *8*, 987. [[CrossRef](#)]
60. Kumar, M.; Kumar Patel, M.; Kumar, N.; Bajpai, A.B.; Siddique, K.H.M. Metabolomics and Molecular Approaches Reveal Drought Stress Tolerance in Plants. *Int. J. Mol. Sci.* **2021**, *22*, 9108. [[CrossRef](#)]
61. Li, Y.; Si, Y.-T.; He, Y.-X.; Li, J.-X. Comparative Analysis of Drought-Responsive and -Adaptive Genes in Chinese Wingnut (*Pterocarya stenoptera* C. DC). *BMC Genom.* **2021**, *22*, 155. [[CrossRef](#)] [[PubMed](#)]
62. Fu, L.; Wu, D.; Zhang, X.; Xu, Y.; Kuang, L.; Cai, S.; Zhang, G.; Shen, Q. Vacuolar H⁺-Pyrophosphatase HVP10 Enhances Salt Tolerance via Promoting Na⁺ Translocation into Root Vacuoles. *Plant Physiol.* **2022**, *188*, 1248–1263. [[CrossRef](#)] [[PubMed](#)]
63. Wang, Y.; Chen, G.; Zeng, F.; Han, Z.; Qiu, C.; Zeng, M.; Yang, Z.; Xu, F.; Wu, D.; Deng, F.; et al. Molecular Evidence for Adaptive Evolution of Drought Tolerance in Wild Cereals. *New Phytol.* **2023**, *237*, 497–514. [[CrossRef](#)] [[PubMed](#)]
64. Wheeler, T.J.; Eddy, S.R. Nhmmer: DNA Homology Search with Profile HMMs. *Bioinformatics* **2013**, *29*, 2487–2489. [[CrossRef](#)] [[PubMed](#)]
65. Finn, R.D.; Bateman, A.; Clements, J.; Coggill, P.; Eberhardt, R.Y.; Eddy, S.R.; Heger, A.; Hetherington, K.; Holm, L.; Mistry, J.; et al. Pfam: The Protein Families Database. *Nucl. Acids Res.* **2014**, *42*, D222–D230. [[CrossRef](#)] [[PubMed](#)]
66. Chen, C.; Chen, H.; Zhang, Y.; Thomas, H.R.; Frank, M.H.; He, Y.; Xia, R. TBtools: An Integrative Toolkit Developed for Interactive Analyses of Big Biological Data. *Mol. Plant* **2020**, *13*, 1194–1202. [[CrossRef](#)]
67. Colmsee, C.; Beier, S.; Himmelbach, A.; Schmutzer, T.; Stein, N.; Scholz, U.; Mascher, M. BARLEX—The Barley Draft Genome Explorer. *Mol. Plant* **2015**, *8*, 964–966. [[CrossRef](#)]
68. Bolser, D.M.; Staines, D.M.; Perry, E.; Kersey, P.J. Ensembl Plants: Integrating Tools for Visualizing, Mining, and Analyzing Plant Genomic Data. In *Plant Genomics Databases*; Van Dijk, A.D.J., Ed.; Methods in Molecular Biology; Springer: New York, NY, USA, 2017; Volume 1533, pp. 1–31. ISBN 978-1-4939-6656-1.
69. Letunic, I.; Khedkar, S.; Bork, P. SMART: Recent Updates, New Developments and Status in 2020. *Nucl. Acids Res.* **2021**, *49*, D458–D460. [[CrossRef](#)]
70. Horton, P.; Park, K.-J.; Obayashi, T.; Fujita, N.; Harada, H.; Adams-Collier, C.J.; Nakai, K. WoLF PSORT: Protein Localization Predictor. *Nucl. Acids Res.* **2007**, *35*, W585–W587. [[CrossRef](#)]
71. Duvaud, S.; Gabella, C.; Lisacek, F.; Stockinger, H.; Ioannidis, V.; Durinx, C. Expasy, the Swiss Bioinformatics Resource Portal, as Designed by Its Users. *Nucl. Acids Res.* **2021**, *49*, W216–W227. [[CrossRef](#)]
72. Bannai, H.; Tamada, Y.; Maruyama, O.; Nakai, K.; Miyano, S. Extensive Feature Detection of N-Terminal Protein Sorting Signals. *Bioinformatics* **2002**, *18*, 298–305. [[CrossRef](#)]
73. Kumar, S.; Stecher, G.; Tamura, K. MEGA7: Molecular Evolutionary Genetics Analysis Version 7.0 for Bigger Datasets. *Mol. Biol. Evol.* **2016**, *33*, 1870–1874. [[CrossRef](#)] [[PubMed](#)]
74. He, Z.; Zhang, H.; Gao, S.; Lercher, M.J.; Chen, W.-H.; Hu, S. Evolvview v2: An Online Visualization and Management Tool for Customized and Annotated Phylogenetic Trees. *Nucl. Acids Res.* **2016**, *44*, W236–W241. [[CrossRef](#)] [[PubMed](#)]
75. Lescot, M. PlantCARE, a Database of Plant Cis-Acting Regulatory Elements and a Portal to Tools for in Silico Analysis of Promoter Sequences. *Nucl. Acids Res.* **2002**, *30*, 325–327. [[CrossRef](#)] [[PubMed](#)]
76. Livak, K.J.; Schmittgen, T.D. Analysis of Relative Gene Expression Data Using Real-Time Quantitative PCR and the 2^{- $\Delta\Delta$ Ct} Method. *Methods* **2001**, *25*, 402–408. [[CrossRef](#)]

Disclaimer/Publisher’s Note: The statements, opinions and data contained in all publications are solely those of the individual author(s) and contributor(s) and not of MDPI and/or the editor(s). MDPI and/or the editor(s) disclaim responsibility for any injury to people or property resulting from any ideas, methods, instructions or products referred to in the content.